GAKUTO International Series
Mathematical Sciences and Applications, Vol.**(2010)
Current Advances in Nonlinear Analysis and Related Topics, pp.43–60

A MACROSCOPIC MODEL FOR PEDESTRIAN FLOWS IN PANIC SITUATIONS

Rinaldo M. Colombo
Department of Mathematics, Brescia University
via Branze 28, I-25123 Brescia, Italy
E-mail: rinaldo@ing.unibs.it

Paola Goatin
IMATH, Université du Sud Toulon-Var
BP. 56, 83162 La Valette du Var Cedex, France
E-mail: goatin@univ-tln.fr

and

Massimiliano D. Rosini
ICM, Warsaw University
Pawinskiego 5a, 02-106 Warszawa, Poland
E-mail: mrosini@icm.edu.pl

Abstract. In this paper we present the macroscopic model for pedestrian flows proposed by Colombo and Rosini [10] and show its main properties. In particular, this model is able to properly describe the movements of crowds, even after panic has arisen. Furthermore, it is able to reproduce the so called Braess' paradox for pedestrians. From the mathematical point of view, it provides one of the few examples of non classical shocks motivated by real problems, for which a global existence result is available. Finally, its assumptions were experimentally confirmed by an empirical study of a crowd crush on the Jamarat Bridge in Mina, Saudi Arabia, near Mecca, see [17].

AMS Subject Classification 35L65, 90B20.

1 Introduction

In the sociological literature [3, 15, 28, 34, 42], *panic* is considered as a sudden terror which dominates or replaces thinking. Both animals and humans are vulnerable to panic. Panic is infectious, in the sense that one individual's panic may easily spread to other members of the group nearby and soon to the entire group. It typically occurs in disaster or violent situations. It is believed to originate from biological responses in the brains and endocrine systems, for instance in the case of herd animals as the response to predators. Often, a large stampede eliminates everything along its path, possibly including some individuals of the escaping group, too. Deaths from stampedes occur primarily from compressive asphyxiation, and usually not from trampling. These accidents are referred to as crowd crushes. At the individual level, warning signs of an incumbent crowd crush include the rise of density to roughly more than four people per square meter.

Since decades, the needs of emergency services and armed forces around the world have been posing several requests to engineers, architects, sociologists, ... aiming at the prevention or, at least, at a rational management of panic. We recall that the worst recorded stampede in history took place in Chongqing, China, during World War II. A bombing of the city on June 6th, 1941, triggered mass panic in an air raid shelter, killing approximately 4,000 people, most of them by suffocation, see [35] for an analysis of the post–traumatic responses to aerial bombing. In the prevention of these tragedies, desing and planning have an essential role.

At the design and planning levels, engineers and architects try to prevent the possible rise of panic, usually by preventing congestion locations and determining the most efficient escape routes. In fact, pedestrians evacuating a closed space accumulate near to door exits. The rise of panic may create a dramatic fall in the overall people outflow. The most effective methods adopted to speed up the evacuation of a large room are often nonintuitive. For instance, a tall column placed in front of the door exit, may be helpful, as the obstacle reduces the inter–pedestrian pressure in front of the door, decreasing the magnitude of clogging and making the overall outflow higher and more regular. This is known as the *Braess' paradox* for pedestrian flows. Optimal management problems about the shape and the position of such obstacle are crucial issues, but still not completely clear and still under investigation.

Modern developments may help prevent some of the approximately two thousand deaths that annually occur in accidents owing to crowding. In Table 1 we give a non–exhaustive survey of the main crowd accidents. Human stampedes most often occur during religious pilgrimages, professional sporting and music events. They also often occur in times of mass panic, as a result of a fire or explosion, as people try to get away.

The increasing interest for pedestrian flows is testified by the growing number of papers published in international journals. In Figure 1, it is represented a non–exhaustive survey of the number of papers having in the title the word "pedestrian" and published in Elsevier or Springer journals versus year. Often, these models are of a microscopic nature, i.e. they postulate some rules for the behavior of each individual and then consider many individuals, as in [16, 18, 19, 21, 22, 25, 33, 36, 37, 38, 41]. Fewer articles develop continuum, or macroscopic, models, where pedestrians are treated in an aggregate way and detailed interactions are overlooked, as for instance in [1, 2, 11, 13, 23, 24, 29, 40].

YEAR	DEAD	CITY	NATION	YEAR	DEAD	CITY	NATION
1872	19	Ostrów Wielkopolski	Poland	1999	53	Minsk	Belarus
1876	278	Brooklyn	USA	2001	43	Henderson	USA
1883	12	Brooklyn	USA	2001	126	Accra	Ghana
1883	180	Sunderland	England	2001	7	Sofia	Bulgaria
1896	1,389	Moscow	Russia	2003	21	Chicago	USA
1908	16	Barnsley	England	2003	100	West Warwick	USA
1913	73	Michigan	USA	2004	194	Buenos Aires	Argentina
1943	173	London	England	2004	251	Mecca	Saudi Arabia
1956	124	Yahiko	Japan	2005	300	Wai	India
1971	66	Glasgow	England	2005	265	Maharashtra	India
1979	11	Cincinnati	USA	2005	1,000	Baghdad	Iraq
1982	66	Luzhniki	Russia	2006	345	Mecca	Saudi Arabia
1985	39	Brussels	Belgium	2006	74	Pasig City	Philippines
1989	96	Sheffield	England	2006	51	Ibb	Yemen
1990	1426	Al-Mu'aysam	Saudi Arabia	2007	12	Chililabombwe	Zambia
1991	40	Orkney	South Africa	2008	12	Mexico City	Mexico
1993	21	Hong Kong	Cina	2008	23	Omdurman	Sudan
1993	73	Madison	USA	2008	147	Jodhpur	India
1994	270	Mecca	Saudi Arabia	2008	162	Himachal Pradesh	India
1996	82	Guatemala City	Guatemala	2008	147	Jodhpur	India
1998	70	Kathmandu	Nepal	2008	1	New York	USA
1998	119	Mecca	Saudi Arabia	2009	19	Abidjan	Côte d'Ivoire

Table 1: A list with the main crowd accidents occurred in the recent years in the world.

However, microscopic approaches are computationally expensive, as each individual is represented by an ordinary differential equation to be solved at each time step, and as the number of individuals increases, so does the size of the system to be solved. On the other hand, the macroscopic models are computationally less expensive because they have fewer design details in terms of interaction among the pedestrians and between the pedestrians and their environment. Thus, it is desirable to use macroscopic models if a good model can be found satisfactorily to describe the pedestrian flows. In addition, only the availability of good continuum models allows to state and possibly solve optimal management problems. In fact, the aim of a good macroscopic model is to capture features of real pedestrian flows and to reproduce them within an analytically treatable framework.

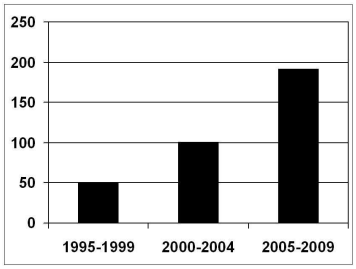

Figure 1: Number of papers having in the title the word "pedestrian" and published in Elsevier or Springer journals versus year.

The understanding and modeling of the multi–scale and multi–physic phenomena involved by crowd–structure interaction make a contribution from different research field necessary to achieve general and conclusive results. For instance, the pedestrian walking behavior has been extensively studied in the field of biomechanics, while the crowd

modeling belongs to transportation, physics and applied mathematics research fields and the structural design of efficient facilities for pedestrians to civil engineering. The convergence of these multidisciplinary knowledges would represent a significant advance in the comprehension of the phenomena involved in pedestrian flows.

Applications related to civil engineering and architecture have been among the main practical motivations and final goals of these studies. A recent issue considered arises by the onset of panic conditions, which substantially modify the crowd dynamics. Therefore, the design of structures, such as stadia grandstands or public buildings, cannot be simply based on normal crowd conditions. Indeed, crowd behavior in panic have to be taken into account both for evacuation purpose and to prevent the structural collapse due to congestion phenomena.

Another difficulty in modeling pedestrians movements derive from their behavior of living systems. It is well understood, in the case of crowd, that human and animal behavior follow specific strategies that modify laws of classical mechanics. This is a specific characteristic of all living systems even in the case of low scales such as insects or cells. Therefore, the coupling of living and mechanical systems have to be taken into account in a comprehensive modeling approach. It is worth to recall the two main different aspects which characterize these two type of systems. First, mechanical systems follow rules of continuum mechanics according to conservation laws and are constant in time; while living systems follow rules generated by their self–organized ability in responding the contingent situations. Second, a mechanical system is represented by continuum models, namely by a system with an infinite number of freedom; while a living system is a discrete system, that is, a system with finite degrees of freedom.

Aim of this paper is to describe the actually unique macroscopic model capable to predict the crowd behavior in panic situations and proposed by Colombo and Rosini in [10] and investigated in [8, 9, 12, 13, 17, 29, 30, 32, 39, 43]. The paper develops in five more sections. Section 2 is addressed to describe the real situations that we want to model and to explain why the classical theory can not be useful. Section 3 is devoted to define a proper non–classical Riemann solver, while Section 4 is devoted to analyze the Cauchy problem. Applications of the model are discussed in Section 5, pointing out cases in which the Braess' paradox occurs. Finally, conclusions are discussed in the last section.

2 The Need of a Non–Classical Theory

The situation that we want to describe is the evacuation of pedestrians from a narrow corridor or a bridge, mathematically represented by the interval $[0, D]$. It is assumed that the escaping pedestrians have to pass through an exit, *"door"* sited at D. Before reaching it, they have to go through an *"obstacle"* at, say, d whose role is to regulate the evcuation process. The model should provide reasonable answers to the following questions:

Panic: When, where, how and why does panic arise?

Clog doors: When, how and why does the efficiency of the exit fall down?

Braess' paradox: When, how and why is the obstacle helpful in the evacuation?

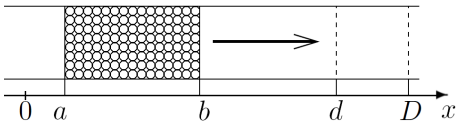

Figure 2: Evacuation of a corridor $[0, D]$ through the exit door at D. The obstacle at d regulates the flow. At the initial time pedestrians are uniformly distributed in $[a, b]$.

Obviously, the total number of pedestrians is conserved. We also assume that the average velocity v of the pedestrians at time t and location x is a function of the crowd density $\rho(t, x)$, namely $v = v(\rho)$, so that the crowd flow is $f(\rho) = \rho\, v(\rho)$. Then, we are led to the conservation law

$$\partial_t \rho + \partial_x f(\rho) = 0\,, \tag{2.1}$$

analogous to the classical Lighthill–Whitham [27] and Richards [31] model.

One might be now lead to force pedestrian flow to follow the same description provided in the case of vehicular traffic by the classical LWR model. This would amount first to introduce also for pedestrians a speed law and a fundamental diagram, roughly speaking, such as those in Figure 3. Then, the standard classical definitions of entropy solutions [5,

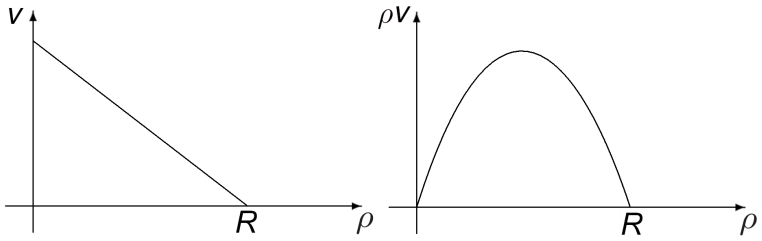

Figure 3: The speed law and the fundamental diagram used in the classical LWR [27, 31] model for vehicle traffic.

14] could be applied. However, the resulting model would not be able to capture relevant patterns that are typical of crowd dynamics and that are not present in vehicular traffic. In particular, the resulting description of the behavior of pedestrians in panic situations would be hardly acceptable. More than that, the very definition of *panic* would be difficult.

From the analytical point of view, we stress that classical solutions to (2.1) satisfy the maximum principle, see [14, Theorem 6.2.2] or [26, Chapter IV, Theorem 2.1(a)]. This elementary analytical result prevents any increase in the maximal density, in contrast with a realistic description of panic, where a sort of *overcompression* arises in panic situation and is often a cause of major accidents.

The model proposed by Colombo and Rosini in [10] relies on an extension of the interval of the possible crowd densities: beyond the interval $[0, R]$ of the standard densities they introduced the *panic states* $]R\,, R^*]$. Therefore, the speed law and the fundamental diagram proposed in in [10] are those here displayed in Figure 4. However, to avoid the implications of the maximum principle, also the very definition of solution needs to be suitably modified, as described below.

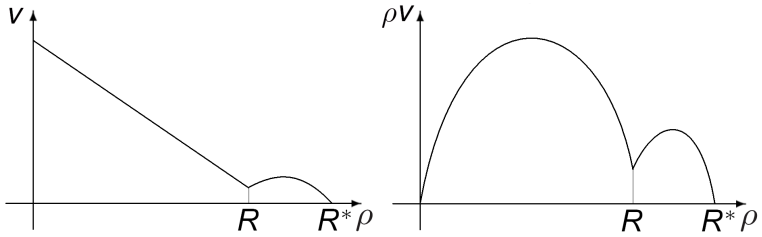

Figure 4: The speed law and the fundamental diagram used in [10] to model pedestrian flows.

3 The Riemann Problem

In this section we present the non–classical Riemann solver introduced in [10] and its main properties. Recall first that by *Riemann Problem* for (2.1) we mean the particular Cauchy problem for (2.1) with an initial datum that attains only two values. More precisely, the Riemann Problem for (2.1) is

$$\begin{cases} \partial_t \rho + \partial_x f(\rho) = 0 \\ \rho(0,x) = \begin{cases} \rho^l & \text{if } x < 0 \\ \rho^r & \text{if } x > 0\,. \end{cases} \end{cases} \tag{3.2}$$

We call *Riemann Solver* for (3.2) the map $\mathcal{R}$ that associates to any pair of the initial states ρ^l, ρ^r the solution $\rho(t,x) = \big(\mathcal{R}(\rho^l,\rho^r)\big)(t,x)$ to (3.2). As is well known, the Riemann Solver contains all the physical information about the solutions to (2.1). Indeed, once $\mathcal{R}$ is known, a constructive analytical procedure that leads to the solution of any Cauchy problem (4.6) is available, as soon as $\bar\rho$ has bounded variation, see for instance [6, 7, 20].

The definition of $\mathcal{R}$ proposed in [10] essentially relies on some qualitative properties of the fundamental diagram in Figure 4. For completeness, we recall here the necessary assumptions on the flux f, together with their physical meaning, as in [12].

(F.1) The Lipschitzeanity of f is a minimal regularity requirement to ensure the finite speed of propagation of the waves:

$$f \in \mathbf{W^{1,\infty}}\left([0,R^*]\,;[0,+\infty[\right)\ .$$

(F.2) The flow vanishes if and only if the density is either zero or maximal:

$$f(\rho) = 0 \text{ if and only if } \rho \in \{0, R^*\}\ .$$

(F.3) Concavity is a standard technical assumption that avoids mixed waves:

$$\text{the restrictions } f_{\big|_{[0,R]}} \text{ and } f_{\big|_{[R,R^*]}} \text{ are strictly concave.}$$

(F.4) The maximal flow in standard situations exceeds that in panic:

$$\max\left\{f(\rho)\colon \rho \in]0,R[\right\} > \max\left\{f(\rho)\colon \rho \in]R\,,R^*[\right\}\ .$$

(F.5) When entering the panic states, there is a small increase in the flow:

$$f \text{ has a local minimum at } R\ .$$

(F.6) The flow $f(R)$, i.e. the flow at the standard maximal density, is very small:

$$f(R) < \min\{q'(R+)R, -q'(R-)(R^* - R)\} \ .$$

As a consequence of the above assumptions, there exist a unique $R_M \in]0, R[$ and a unique $R_M^* \in]R\,, R^*[$ such that

$$f(R_M) = \max\{f(\rho)\colon \rho \in]0, R[\} > f(R_M^*) = \max\{f(\rho)\colon \rho \in]R\,, R^*[\} \ .$$

Furthermore, by **(F.6)**, the line through the origin and $(R, f(R))$ intersects $f = f(\rho)$

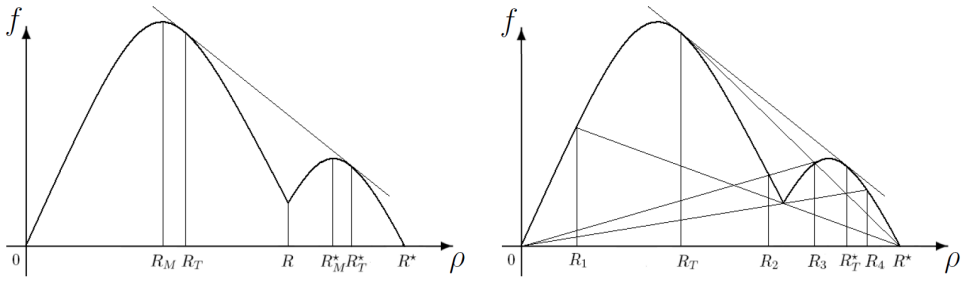

Figure 5: The flow function f and notations.

at a point $(R_4, f(R_4))$ with $R_4 \in]R, R^*[$, while the line through $(R^*, 0)$ and $(R, f(R))$ intersects $f = f(\rho)$ at a point $(R_1, f(R_1))$ with $R_1 \in]0, R[$, see Figure 5, right.
It is of use to further introduce the auxiliary functions ψ and ϕ. First, see Figure 6, let $\psi(R) = R$ and, for $\rho \neq R$, let $\psi(\rho)$ be such that the straight line through $(\rho, f(\rho))$ and $(\psi(\rho), f(\psi(\rho)))$ is tangent to the graph of f at $(\psi(\rho), f(\psi(\rho)))$. By **(F.6)**, ψ is well

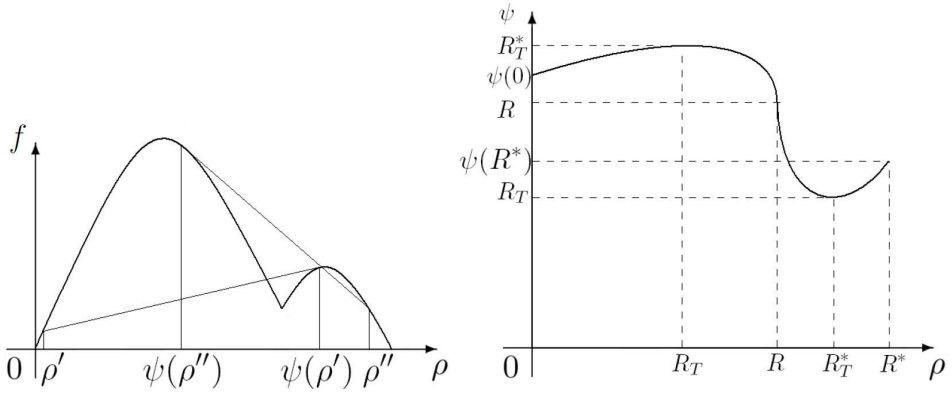

Figure 6: The function ψ: its geometrical meaning, left, and its graph, right.

defined and $\psi(\rho) \neq R$ for all $\rho \in [0, R^*] \setminus \{R\}$. We assume also that there exists only one couple $(R_T, R_T^*) \in]R_M, R[\times]R_M^*, R^*[$ such that $\psi(R_T) = R_T^*$ and $\psi(R_T^*) = R_T$, see Figure 5, i.e.

(F.7) $f(\psi(R^*)) < -q'(R^*)\,(R^* - \psi(R^*))$.

Then, the line through $(R_T, f(R_T))$ and $(R_T^*, f(R_T^*))$ is the unique tangent to $f = f(\rho)$ in two (distinct) points. These assumptions imply that ψ is increasing in $[0, R_T[\cup]R_T^*, R^*]$

and decreasing in $]R_T, R_T^*[$ while $\psi'(R_T) = \psi'(R_T^*) = 0$, see Figure 6, right. Moreover, $R_T < \psi(R^*) < R < \psi(0) < R_T^*$.
Finally, we concentrate our attention on the cases in which:

(F.8) $R_T^* < R_4 < R^*$ and $0 < R_1 < R_T$.

(F.9) $[\rho \mapsto \psi(\rho) - \rho]$ is non–increasing in $[0, R]$.

Let $\bar\rho \in [0, R_T[$, then by **(F.6)** the line through $(\bar\rho, f(\bar\rho))$ and $(\psi(\bar\rho), f(\psi(\bar\rho)))$ has a further intersection with the graph of f, which we call $(\phi(\bar\rho), f(\phi(\bar\rho)))$.

Following [10, 12], we now define a non–classical Riemann Solver suited to the description of crowd dynamics, yielding physically reasonable solutions to all Riemann problems of the type (3.2). More precisely, for any pair $(\rho^l, \rho^r) \in [0, R^*]^2$, we denote by $\mathcal{R}(\rho^l, \rho^r)$ the self similar weak solution to the Riemann problem (3.2) computed at time, say, $t = 1$. Introduce two thresholds s and Δs such that

$$s > 0\,,\ \Delta s > 0\,,\ s < R_M \text{ and } R > s + \Delta s \geq \phi(s) > R_T > R - \Delta s\,. \tag{3.3}$$

The solution to Riemann problems with data in $[0, R^*]$ are selected through the following

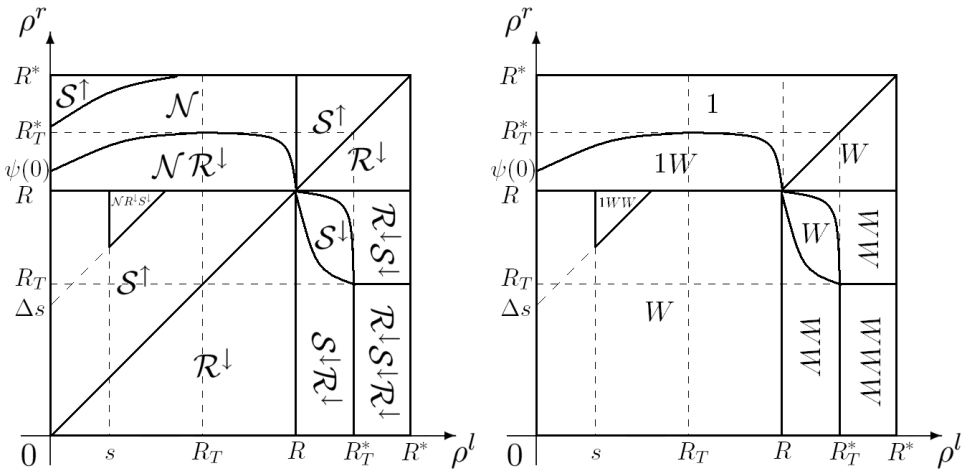

Figure 7: Left: The Riemann solver selected by **(R.1)**–**(R.4)**. Here, $\mathcal{N}\mathcal{R}^\downarrow$ indicates that $\mathcal{R}(\rho^l, \rho^r)$ is a non–classical shock followed by a decreasing rarefaction. Right: The weighted total variation TV_w. The notation $1W$ means that the first wave has weight 1 and the second wave has weight W.

conditions, see Figure 7, left.

(R.1) If $\rho^l, \rho^r \in [0, R]$, then $\mathcal{R}(\rho^l, \rho^r)$ selects the classical solution unless

$$\rho^l > s \quad \text{and} \quad \rho^r - \rho^l > \Delta s\,.$$

In this case, $\mathcal{R}(\rho^l, \rho^r)$ consists of a non–classical shock between ρ^l and $\psi(\rho^l)$, followed by the classical solution between $\psi(\rho^l)$ and ρ^r.

(R.2) If $\rho^r < \rho^l$, then $\mathcal{R}(\rho^l, \rho^r)$ is the classical solution.

(R.3) If $R \leq \rho^l < \rho^r$ or $\rho^l < R < \rho^r$ and the segment between $(\rho^l, f(\rho^l))$ and $(\rho^r, f(\rho^r))$ does not intersect $f = f(\rho)$, then the solution is a shock between ρ^l and ρ^r.

(R.4) If $\rho^l < R < \rho^r$ and the segment between $(\rho^l, f(\rho^l))$ and $(\rho^r, f(\rho^r))$ intersects $f = f(\rho)$, then $\mathcal{R}(\rho^l, \rho^r)$ consists of a non–classical shock between ρ^l and a panic state followed by a possibly null classical wave. More precisely,

$\rho^r \in \left]R\,, \psi(\rho^l)\right[$: $\mathcal{R}(\rho^l, \rho^r)$ consists of a non–classical shock between ρ^l and $\psi(\rho^l)$, followed by a decreasing rarefaction between $\psi(\rho^l)$ and ρ^r;

$\rho^r \in \left[\psi(\rho^l), R^*\right[$: $\mathcal{R}(\rho^l, \rho^r)$ consists of a single non–classical shock.

We recall here the main result of [10, Theorem 2.1] concerning the solution to Riemann problems. To state it, the following subsets of the square $[0, R^*]^2$ are of use, see Figure 7.

$$\begin{aligned}
\mathcal{C}_{\mathcal{N}} &= \left\{(\rho^l, \rho^r) \in [0, R^*]^2 \colon \rho^l \geq \rho^r \geq R\right\} \\
\mathcal{N}_{\mathcal{C}} &= \left\{(\rho^l, \rho^r) \in [0, R]^2 \colon \rho^l > s \text{ and } \rho^r - \rho^l > \Delta s\right\} \\
\mathcal{C} &= ([0, R^*] \times [0, R[) \cup \mathcal{C}_{\mathcal{N}} \setminus \mathcal{N}_{\mathcal{C}} \\
\mathcal{N} &= ([0, R^*] \times]R\,, R^*]) \cup \mathcal{N}_{\mathcal{C}} \setminus \mathcal{C}_{\mathcal{N}}
\end{aligned}$$

Theorem 3.1 ([10, Theorem 2.1], [32, Theorem 2.1, Proposition 3.1])**.** *Let $f \colon [0, R^*] \to [0, +\infty[$ satisfy Assumptions **(F.1)**–**(F.8)**. Choose thresholds s and Δs such that* (3.3) *holds. Then, there exists a unique Riemann solver $\mathcal{R} \colon [0, R^*]^2 \to \mathbf{BV}(\mathbb{R})$ satisfying **(R.1)**–**(R.4)** and such that $\rho(t, x) = \big(\mathcal{R}(\rho^l, \rho^r)\big)(x/t)$ is a weak solution to* (3.2)*. Moreover,*

- *$\mathcal{R}$ is consistent in $\mathring{\mathcal{C}}$ and separately, in $\mathcal{N}$,*
- *$\mathcal{R}$ is $\mathbf{L^1_{loc}}$-continuous in $\mathring{\mathcal{C}}$, in $\mathcal{N}$ and also along the segment $\rho^l = \rho^r$ for $\rho^l \in]R\,, R^*]$.*

Recall that a Riemann Solver $\tilde{R}$ is *consistent* if the following two conditions hold.

$$\textbf{(C.1)} \quad \left.\begin{array}{ll} \tilde{R}(u^l, u^m)(\bar{x}) & = u^m \\ \tilde{R}(u^m, u^r)(\bar{x}) & = u^m \end{array}\right\} \quad \Rightarrow \quad \tilde{R}(u^l, u^r) = \left\{\begin{array}{ll} \tilde{R}(u^l, u^m) & \text{if } x < \bar{x} \\ \tilde{R}(u^m, u^r) & \text{if } x \geq \bar{x} \end{array}\right.$$

$$\textbf{(C.2)} \quad \tilde{R}(u^l, u^r)(\bar{x}) = u^m \quad \Rightarrow \quad \left\{\begin{array}{l} \tilde{R}(u^l, u^m) = \left\{\begin{array}{ll} \tilde{R}(u^l, u^r) & \text{if } x \leq \bar{x} \\ u^m & \text{if } x > \bar{x} \end{array}\right. \\ \tilde{R}(u^m, u^r) = \left\{\begin{array}{ll} u^m & \text{if } x < \bar{x} \\ \tilde{R}(u^l, u^r) & \text{if } x \geq \bar{x} \end{array}\right. \end{array}\right.$$

Essentially, **(C.1)** states that whenever two solutions to two Riemann problems can be placed side by side, then their juxtaposition is again a solution to a Riemann problem, see Figure 8. **(C.2)** is the viceversa. Both these properties are enjoyed by the standard Lax solver. Moreover, if the Riemann solver $\tilde{R}$ generates a standard Riemann semigroup, then $\tilde{R}$ needs to satisfy **(C.1)**.

Proposition 3.2 ([32, Proposition 3.2])**.** *The Riemann solver $\mathcal{R}$ satisfies* **(C.2)** *but not* **(C.1)** *in $[0, R^*]^2$.*

Proof. In order to prove that $\mathcal{R}$ satisfies **(C.2)** in $[0, R^*]^2$ it is sufficient to consider the following two cases.

- $\rho^l < R < \rho^r < \rho^m < \psi(\rho^l)$

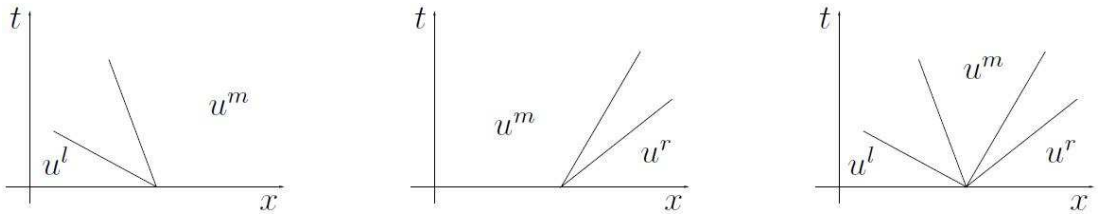

Figure 8: Consistency of a Riemann solver.

- $s < \rho^l < \rho^r - \Delta s$, $\rho^r < R$ and $\psi(\rho^r) < \rho^m < \psi(\rho^l)$

Easily, the reader can check that in both cases **(C.2)** is satisfied. Finally, if $\rho^l, \rho^m, \rho^r \in [0, R^*]^2$ satisfy one of the following conditions, then **(C.1)** is not satisfied.

- $\rho^l, \rho^m \in [0, R[$, $\mathcal{R}(\rho^l, \rho^m) = \mathcal{S}^{\uparrow}$, $\rho^r > \psi(\rho^l)$ and the line $r(\rho^l, \rho^m)$ has slope less than the line $r(\rho^l, \rho^r)$
- $\rho^l, \rho^m \in [0, R[$, $\mathcal{R}(\rho^l, \rho^m) = \mathcal{S}^{\uparrow}$, $R < \rho^r < \psi(\rho^l)$ and $r(\rho^l, \rho^m)$ has slope less than the line $r(\rho^l, \psi(\rho^l))$
- $\rho^l, \rho^r \in [0, R[$, $\mathcal{R}(\rho^l, \rho^r) = \mathcal{S}^{\uparrow}$ and $\psi(\rho^r) < \rho^m = \psi(\rho^l)$

□

Proposition 3.3 ([32, Proposition 3.3])**.** *$\mathcal{R}$ is not $\mathbf{L^1_{loc}}$-continuous in $[0, R^*]^2$.*

Proof. Fix $\epsilon > 0$. If $\rho^l, \rho_1^r, \rho_2^r \in [0, R^*]^2$ with $\rho_2^r - \rho_1^r < \epsilon$ and satisfy one of the following conditions, then $\lim_{\epsilon \to 0+} \left\| \mathcal{R}(\rho^l, \rho_2^r) - \mathcal{R}(\rho^l, \rho_1^r) \right\|_{\mathbf{L^1}} \neq 0$.

- $\rho^l \leq s < \rho_1^r < R < \rho_2^r$
- $s < \rho^l < s + \Delta s < \rho_1^r < \rho^l + s < \rho_2^r < R$
- $s + \Delta s \leq \rho^l < \rho_1^r < R < \rho_2^r$

Finally, if $\rho^r, \rho_1^l, \rho_2^l \in [0, R^*]^2$ with $\rho_2^l - \rho_1^l < \epsilon$ satisfy one of the following conditions, then $\lim_{\epsilon \to 0+} \left\| \mathcal{R}(\rho_2^l, \rho^r) - \mathcal{R}(\rho_1^l, \rho^r) \right\|_{\mathbf{L^1}} \neq 0$

- $\rho_1^l < s \leq \rho_2^l < \rho^r - \Delta s$ and $\rho^r < R$
- $\rho_1^l < \rho^r - \Delta s \leq \rho_2^l < R$

□

For any fixed constant $W > 1$, let the weighted total variation $\mathrm{TV_w} \colon \mathbf{BV}(\mathbb{R}; \mathbb{R}) \to [0, +\infty[$ defined as it follows, see Figure 7, right. Let $\mathcal{R}(\rho^l, \rho^r)$ be a single wave, then

- $\mathrm{TV_w}(\mathcal{R}(\rho^l, \rho^r)) = \left| \rho^r - \rho^l \right|$ if $\mathcal{R}(\rho^l, \rho^r)$ is a classical or non–classical shock with $\rho^r \in]R, R^*]$;
- $\mathrm{TV_w}(\mathcal{R}(\rho^l, \rho^r)) = W \cdot \left| \rho^r - \rho^l \right|$ otherwise, i.e. if $\rho^r \leq R$ or $\rho^r < \rho^l$.

Proposition 3.4 ([32, Proposition 5.1])**.** *Assume that*

$$\frac{\phi(0)}{\psi(0)} \leq \frac{\Delta s}{\psi(s) - s}\,, \tag{3.4}$$

and consider a constant W such that

$$W > 1 \quad \text{and} \quad \frac{\phi(0)}{\psi(0)} \leq \frac{W+1}{2W} \leq \frac{\Delta s}{\psi(s) - s}\,. \tag{3.5}$$

Then, TV_{w} *does not increase after any interaction.*

The theory of classical Riemann solver, see for instance [5, 14], ensures that, in the present scalar case, the total variation of the solution does not increase after any interaction among classical waves. Thus, the proof follows by the analysis of all the possible wave interactions in which non–classical shocks are involved, see [32, Section 5].

4 The Cauchy Problem

In this section we prove an existence results for the Cauchy problem

$$\begin{cases} \partial_t \rho + \partial_x f(\rho) = 0 \\ \rho(0,x) = \bar\rho(x) \end{cases} \tag{4.6}$$

and prove that $\mathcal{R}$ is also not $\mathbf{L^1}$-continuous in $[0, R^*]^2$.

Theorem 4.1 ([12, Theorem 3.4])**.** *Let f satisfy **(F.1)**–**(F.9)**, $s, \Delta s$ satisfy* (3.3) *and assume that there exists a W satisfying* (3.5)*. For any initial datum $\bar\rho \in (\mathbf{L^1} \cap \mathbf{BV})(\mathbb{R}; [0, R^*])$, the Cauchy problem* (4.6) *admits a non–classical weak solution $\rho = \rho(t,x)$ generated by the non–classical Riemann solver $\mathcal{R}$ and defined for all $t \in \mathbb{R}_+$. Moreover:*

$$\mathrm{TV}\left(\rho(t)\right) \leq W \cdot \mathrm{TV}(\bar\rho)\,, \qquad \text{for all } t \in \overline{\mathbb{R}}_+\,. \tag{4.7}$$

Proof. The proof is based on the wave front tracking method [6, 7, 20]. Here we give a sketch for the proof, deferring the details to [12]. As a first step, we fix a mesh $\mathcal{M}_n =$

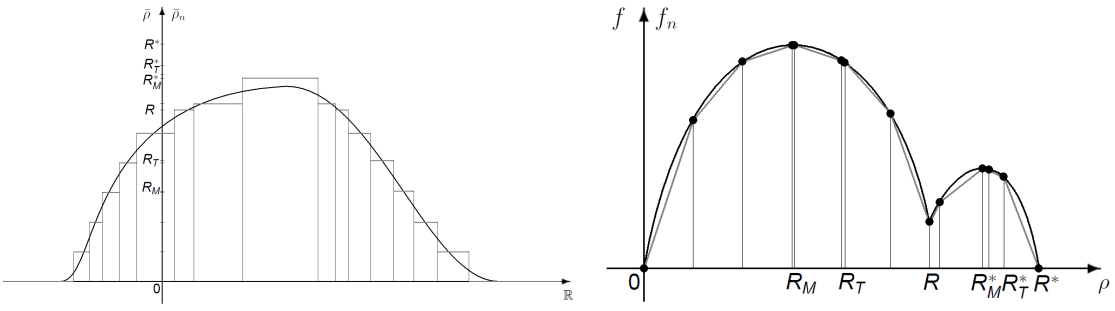

Figure 9: Approximation of the initial data, left, and of the flux, right.

$\{i2^{-n}R^* \,:\, i = 0, 1, \ldots, 2^n\} \cup \{R_M, R_T, R, R_M^*, R_T^*\}$; introduce an approximation f_n in

the set of piecewise linear function such that $f_n(\rho) = f(\rho)$ for all $\rho \in \mathcal{M}_n$; introduce an approximation $\bar\rho_n$ of the initial data $\bar\rho$ in the set of piecewise constant function with compact support and with values in $\mathcal{M}_n$, such that $\mathrm{TV}(\bar\rho_n) \leq \mathrm{TV}(\bar\rho)$ and $\bar\rho_n \to \bar\rho$ in $\mathbf{L^1}$, see Figure 10, left. Then, we obtain the following approximate Cauchy problem.

$$\begin{cases} \partial_t \rho_n + \partial_x f_n(\rho_n) = 0 \\ \rho_n(0,x) = \bar\rho_n(x) \end{cases} \tag{4.8}$$

Solving the Riemann problems associated to each jump of $\bar\rho_n$ and gluing together all these solutions, we obtain the exact solution to (4.8) up to the first time of interaction, see Figure **??**. Solving the corresponding Riemann problem at the first interaction point, it is possible to continue with the construction of the approximating solution ρ_n. This

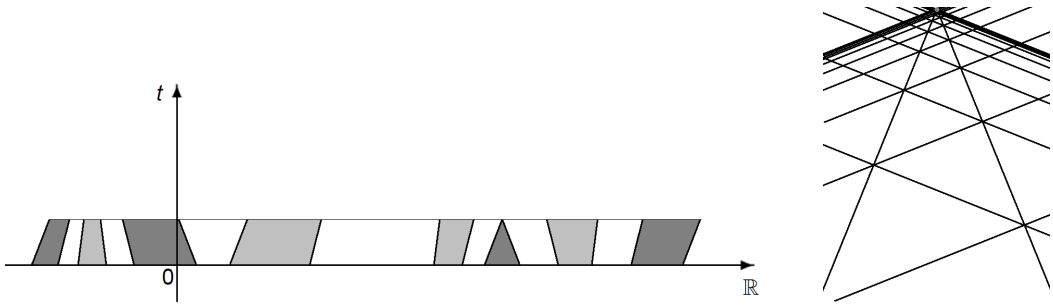

Figure 10: Left: First step for the construction of the solution to (4.8). Right: An example of accumulation point.

procedure can be iterated if there are no accumulation points, see Figure 10, right. By Proposition 3.4, we know that this is not our case and therefore this procedure gives an approximating solution ρ_n for all times. Finally, up to a subsequence, by Helly's theorem the approximating solutions ρ_n converge to a function ρ, which is a solution to (4.6) and satisfies (4.7). □

Proposition 4.2. *$\mathcal{R}$ is not $\mathbf{L^1}$-continuous in $[0, R^*]^2$.*

Proof. Let $n \in \mathbb{N}$ and consider the following Cauchy problems.

$$\begin{cases} \partial_t \rho + \partial_x f(\rho) = 0 \\ \rho(0,x) = \begin{cases} 0 & x \in \,]-\infty, 0[\\ R & x \in [0, +\infty[\end{cases} \end{cases} \quad , \quad \begin{cases} \partial_t \rho_n + \partial_x f(\rho_n) = 0 \\ \rho_n(0,x) = \begin{cases} 0 & x \in \,]-\infty, 0[\\ R + 1/n & x \in [0,1] \\ R & x \in \,]1, +\infty[\end{cases} \end{cases}$$

Easy computations, see Figure 11, show that for all $t > 0$

$$\lim_{n\to\infty} \|\rho(0) - \rho_n(0)\|_{\mathbf{L^1}(\mathbb{R};[0,R^*])} = 0 \text{ and } \lim_{n\to\infty} \|\rho(t) - \rho_n(t)\|_{\mathbf{L^1}(\mathbb{R};[0,R^*])} \neq 0\,,$$

completing the proof. □

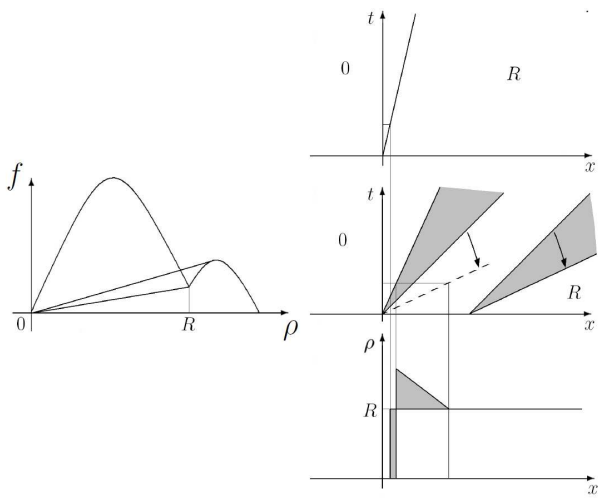

Figure 11: Left: Construction of the solutions ρ and ρ_n to the Cauchy problems considered in the proof of Proposition 4.2. Right, from top to bottom; first diagram, representation of ρ in the (x,t)-plane. Observe that from the origin starts a shock between the densities 0 and R. Second diagram, representation of ρ_n in the (x,t)-plane. Observe that from the origin starts a non–classical shock between the densities 0 and $\psi(0)$ followed by a decreasing rarefaction between the densities $\psi(0)$ and $R+1/n$, while from 1 starts a rarefaction between the densities $R+1/n$ and R. Third diagram, representation of ρ and of the limit ρ_∞ in the (x,ρ)-plane.

5 Application

In this section we apply the model described above to the evacuation of a narrow corridor $[0,D]$. We assume that, at the initial time $t=0$, the crowd is uniformly distributed in $[a,b]\subset[0,D]$, with a relatively high density $\bar\rho\in[R_M,R]$. Consider two doors in d and D, $b<d\le D$, with maximal loads $p,P:\ [0,R^*]\to[0,f(R_M)]$, respectively. High densities at the doors affect on their efficiency, and therefore proper choices of the functions p and P are $p=p_1\ \chi_{[0,R]}+p_2\ \chi_{]R,R^*]}$ and $P=P_1\ \chi_{[0,R]}+P_2\ \chi_{]R,R^*]}$, with $P_2<p_2<P_1<p_1$. Roughly speaking, the first door is larger than the second one, $p>P$, and the high densities of people close to the doors clog them, $p_1>p_2$ and $P_1>P_2$. Let $0<\rho'_D<\rho'_d<\rho''_d<\rho''_D<R$ be such that $f(\rho'_D)=f(\rho''_D)=P_1$ and $f(\rho'_d)=f(\rho''_d)=p_1$. Mathematically, this situation is described by the following Cauchy problem with constraints.

$$\begin{cases} \partial_t\rho+\partial_x f(\rho)=0 & \text{for}\quad t\in\overline{\mathbb{R}}_+,\ x\in[0,D]\\ \rho(0,x)=\bar\rho\ \chi_{[a,b]}(x) & \text{for}\quad x\in[0,D]\\ f\left(\rho(t,d)\right)\le p\left(\rho(t,d)\right) & \text{for}\quad t\in\mathbb{R}_+\\ f\left(\rho(t,D)\right)\le P\left(\rho(t,D)\right) & \text{for}\quad t\in\mathbb{R}_+ \end{cases} \tag{5.9}$$

By applying the wave front tracking method, and solving a certain number of Riemann problems, it is possible to construct a solution of (5.9), see Figure 12, left. Note that pedestrians start exiting through the first door at time $t_I=(d-b)/q'(0)$ and through

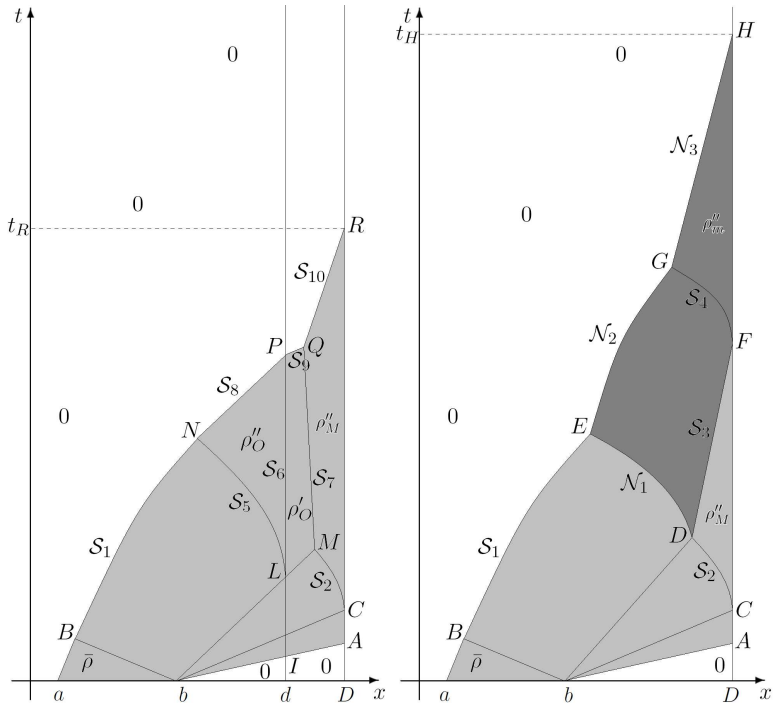

Figure 12: Left, the solution to (5.9), right, the solution to (5.9) without the third equation.

the second door at time $t_A = (D-b)/q'(0)$. At time t_B, the initial shock and rarefaction start to interact, yielding the shock $\mathcal{S}_1$, see Figure 12, left. Due to the interaction, $\mathcal{S}_1$ accelerates while the state to its right decreases.

For certain initial conditions, such as $\bar\rho/(d-b)$ sufficiently large, the outflow through the first door reach its maximal value at time $t_L = (d-b)/q'(\rho'_d)$. A backward shock with support $\mathcal{S}_5$ is formed at L, it interacts with the rarefaction exiting b and accelerates backwards, so that it is bent as in Figure 12, left. Along the right side of $\mathcal{S}_5$ the density is constant and equal to ρ''_d, while on the left side it increases. At time $t_C = (D-b)/q'(\rho'_D)$ the maximal outflow through the second door is reached and appears a backward shock $\mathcal{S}_2$ related to a queue started from the second door. $\mathcal{S}_5$ meets $\mathcal{S}_1$ in N and starts a shock $\mathcal{S}_8$ which reaches the door in P. Therefore, at time t_P all the people have passed through the first door. In Q the shocks started from P and M meet and starts the final shock $\mathcal{S}_{10}$, which meets the second door in R and t_R represents the evacuation time $T(d)$.

In Figure 12, right, the same problem (5.9) is considered, but the first door is removed, i.e. $d \equiv D$. Remarkably, in this particular situation, the evacuation time without the first door is larger than the evacuation time with the first door. The detailed construction of these solutions can be found in [11, Section 4.2].

In particular, changing the position of the first door, namely, letting varying d in $[b, D]$, we obtain the graph for the evacuation time represented in Figure 13. Note that the darker regions in Figure 12, right, represent where the crowd density attains panic values, i.e. $\rho \in \,]R, R^*]$. The presence of the obstacle avoids the density to reach these high values, thus allowing for a faster evacuation of the corridor. Remarkably, there is an interval of values of d such that the presence of the first door helps for the evacuation

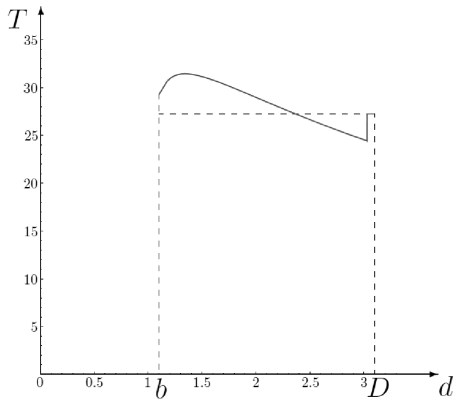

Figure 13: The horizontal dotted line is the evacuation time without the first door. The solid line is the evacuation time, T, as a function of the position of the first door, d.

time, showing that the model properly describe the Braess' paradox for pedestrian flows. Furthermore, it is also clear that the presence of a first door too close to the second one does not have any effect on the evacuation time.

6 Conclusions

We presented the model proposed in [10] and some of its analytical properties. This model can be used to describe real situations, such as a crowd evacuating a corridor. Numerical integrations are possible, allowing a detailed description of the phenomena. Furthermore, the time necessary for people to exit the corridor can be computed.

Reasonable qualitative behaviors of the solutions are described. In particular, the model presented accounts for the possible decrease in the evacuation time thanks to the careful insertion of an obstacle at a well chosen position in front of the exit. This phenomenon, an analog of Braess' paradox [4], is clearly non generic.

Possible criticisms to the model are the fact that it describes only one dimensional movements and the lack of $\mathbf{L^1}$–continuous dependence of the solutions from the initial data. Anyway, it should be reminded that the theory for non–classical shocks and the wave front tracking method are both developed only for the one dimensional case. Secondly, the non–continuous dependence of the solution from the data is due to the presence of the two thresholds s and Δs.

References

[1] N. Bellomo. *Modeling complex living systems.* Modeling and Simulation in Science, Engineering and Technology. Birkhäuser Boston Inc., Boston, MA, 2008. A kinetic theory and stochastic game approach.

[2] N. Bellomo and C. Dogbé. On the modelling crowd dynamics from scaling to hyperbolic macroscopic models. *Math. Models Methods Appl. Sci.*, 18(suppl.):1317–1345, 2008.

[3] R. Berk. *Collective Behavior.* W. C. Brown Co. 1974.

[4] D. Braess, A. Nagurney, and T. Wakolbinger. On a paradox of traffic planning. *Transportation Science*, 39(4):446–450, 2005.

[5] A. Bressan. *Hyperbolic systems of conservation laws*, volume 20 of *Oxford Lecture Series in Mathematics and its Applications*. Oxford University Press, Oxford, 2000. The one-dimensional Cauchy problem.

[6] A. Bressan. The front tracking method for systems of conservation laws. In C. M. Dafermos and E. Feireisl, editors, *Handbook of Partial Differential Equations*. Elsevier, To appear.

[7] A. Bressan and R. M. Colombo. The semigroup generated by 2×2 conservation laws. *Arch. Rational Mech. Anal.*, 133(1):1–75, 1995.

[8] C. Chalons. Numerical approximation of a macroscopic model of pedestrian flows. *SIAM J. Sci. Comput.*, 29(2):539–555 (electronic), 2007.

[9] R. M. Colombo, G. Facchi, G. Maternini, and M. D. Rosini. On the continuum modeling of crowds. *to appear on Proceedings of Symposia in Applied Mathematics*, 2009.

[10] R. M. Colombo and M. D. Rosini. Pedestrian flows and non-classical shocks. *Math. Methods Appl. Sci.*, 28(13):1553–1567, 2005.

[11] R. M. Colombo and M. D. Rosini. Well posedness of balance laws with boundary. *J. Math. Anal. Appl.*, 311(2):683–702, 2005.

[12] R. M. Colombo and M. D. Rosini. Existence of nonclassical solutions in a pedestrian flow model. *Nonlinear Anal. Real World Appl.*, 10(5):2716–2728, 2009.

[13] V. Coscia and C. Canavesio. First-order macroscopic modelling of human crowd dynamics. *Math. Models Methods Appl. Sci.*, 18(suppl.):1217–1247, 2008.

[14] C. M. Dafermos. *Hyperbolic conservation laws in continuum physics*, volume 325 of *Grundlehren der Mathematischen Wissenschaften [Fundamental Principles of Mathematical Sciences]*. Springer-Verlag, Berlin, 2000.

[15] O. Diethelm. The Nosological Position of Panic Reactions. *Am. J. Psychiatry*, 90(6):1295–1316, 1934.

[16] I. Farkas, D. Helbing, and T. Vicsek. Human waves in stadiums. *Phys. A*, 330(1-2):18–24, 2003. Randomness and complexity (Eilat, 2003).

[17] D. Helbing, A. Johansson, and H. Z. Al-Abideen. Dynamics of crowd disasters: An empirical study. *Physical Review E (Statistical, Nonlinear, and Soft Matter Physics)*, 75(4):046109, 2007.

[18] D. Helbing, M. Schönhof, H.-U. Stark, and J. A. Hołyst. How individuals learn to take turns: emergence of alternating cooperation in a congestion game and the prisoner's dilemma. *Adv. Complex Syst.*, 8(1):87–116, 2005.

[19] D. Helbing, J. Siegmeier, and S. Lämmer. Self-organized network flows. *Netw. Heterog. Media*, 2(2):193–210 (electronic), 2007.

[20] H. Holden and N. H. Risebro. *Front tracking for hyperbolic conservation laws*, volume 152 of *Applied Mathematical Sciences*. Springer-Verlag, New York, 2002.

[21] S. Hoogendoorn and P. H. L. Bovy. Simulation of pedestrian flows by optimal control and differential games. *Optimal Control Appl. Methods*, 24(3):153–172, 2003.

[22] S. Hoogendoorn and P. H. L. Bovy. Pedestrian route-choice and activity scheduling theory and models. *Transp. Res. B*, (38):169–190, 2004.

[23] R. L. Hughes. A continuum theory for the flow of pedestrians. *Transportation Research Part B*, 36:507–535, 2002.

[24] R. L. Hughes. The flow of human crowds. In *Annual review of fluid mechanics, Vol. 35*, pages 169–182. Annual Reviews, Palo Alto, CA, 2003.

[25] A. Johansson, D. Helbing, and P. K. Shukla. Specification of the social force pedestrian model by evolutionary adjustment to video tracking data. *Adv. Complex Syst.*, 10(suppl. 2):271–288, 2007.

[26] P. G. Lefloch. *Hyperbolic systems of conservation laws.* Lectures in Mathematics ETH Zürich. Birkhäuser Verlag, Basel, 2002. The theory of classical and nonclassical shock waves.

[27] M. J. Lighthill and G. B. Whitham. On kinematic waves. II. A theory of traffic flow on long crowded roads. *Proc. Roy. Soc. London. Ser. A.*, 229:317–345, 1955.

[28] C. McPhail. *The Myth of the Madding Crowd.* Walter de Gruyter. New York, 1991.

[29] B. Piccoli and A. Tosin. Time-evolving measures and macroscopic modeling of pedestrian flow. Preprint, arXiv:0811.3383v1. Submitted.

[30] B. Piccoli and A. Tosin. Pedestrian flows in bounded domains with obstacles. *Continuum Mechanics and Thermodynamics*, (21):85–107, 2009.

[31] P. I. Richards. Shock waves on the highway. *Operations Res.*, 4:42–51, 1956.

[32] M. D. Rosini. Nonclassical interactions portrait in a macroscopic pedestrian flow model. *J. Differential Equations*, 246(1):408–427, 2009.

[33] A. Schadschneider, A. Kirchner, and K. Nishinari. Cellular automata simulation of collective phenomena in pedestrian dynamics. In *Interface and transport dynamics*, volume 32 of *Lect. Notes Comput. Sci. Eng.*, pages 390–405. Springer, Berlin, 2003.

[34] N. Smelser. *Theory of Collective Behavior.* Free Pres, Nnew York, 1962.

[35] D. J. Somasundaram. Post-traumatic responses to aerial bombing. *Social Science & Medicine*, 42(11):1465–1471, 1996.

[36] Y. Sugiyama and A. Nakayama. Modeling, simulation and observations for freeway traffic and pedestrian. In *Interface and transport dynamics*, volume 32 of *Lect. Notes Comput. Sci. Eng.*, pages 406–421. Springer, Berlin, 2003.

[37] Y. Tajima and T. Nagatani. Scaling behavior of crowd flow outside a hall. *Physica A*, 292:545–554, 2001.

[38] K. Takimoto and T. Nagatani. Spatio-temporal distribution of escape time in evacuation process. *Physica A*, 320:611–621, 2003.

[39] F. Venuti and L. Bruno. Crowd-structure interaction in lively footbridges under synchronous lateral excitation: A literature review. *Physics of Life Reviews*, In Press, Corrected Proof:–, 2009.

[40] F. Venuti, L. Bruno, and N. Bellomo. Crowd dynamics on a moving platform: mathematical modelling and application to lively footbridges. *Math. Comput. Modelling*, 45(3-4):252–269, 2007.

[41] W. Yu and A. Johansson. Modeling crowd turbulence by many-particle simulations. *Physical Review E (Statistical, Nonlinear, and Soft Matter Physics)*, 76(4):046105, 2007.

[42] W. Zhen, L. Mao, and Z. Yuan. Analysis of trample disaster and a case study mihong bridge fatality in china in 2004. *Safety Science*, 46(8):1255–1270, 2008.

[43] X. Zheng, T. Zhong, and M. Liu. Modeling crowd evacuation of a building based on seven methodological approaches. *Building and Environment*, 44(3):437 – 445, 2009.